

Components of wind -tunnel analysis using force balance test data

T.C. Eric Ho^{*1}, Un Yong Jeong^{2a} and Peter Case^{1b}

¹The Boundary Layer Wind Tunnel Laboratory, The University Of Western Ontario, London, Ontario, Canada

²Gradient Wind Engineering Inc., Ottawa, Ontario, Canada

(Received July 27, 2010, Revised December 20, 2012, Accepted January 27, 2013)

Abstract. Since its development in the early 1980's the force balance technique has become a standard method in the efficient determination of structural loads and responses. Its usefulness lies in the simplicity of the physical model, the relatively short records required from the wind tunnel testing and its versatility in the use of the data for different sets of dynamic properties. Its major advantage has been the ability to provide results in a timely manner, assisting the structural engineer to fine-tune their building at an early stage of the structural development. The analysis of the wind tunnel data has evolved from the simple un-coupled system to sophisticated methods that include the correction for non-linear mode shapes, the handling of complex geometry and the handling of simultaneous measurements on multiple force balances for a building group. This paper will review some of the components in the force balance data analysis both in historical perspective and in its current advancement. The basic formulation of the force balance methodology in both frequency and time domains will be presented. This includes all coupling effects and allows the determination of the resultant quantities such as resultant accelerations, as well as various load effects that generally were not considered in earlier force balance analyses. Using a building model test carried out in the wind tunnel as an example case study, the effects of various simplifications and omissions are discussed.

Keywords: wind tunnel test; tall buildings; force balance; time domain analysis; frequency domain analysis

1. Introduction

Before the development of the force balance technique, structural wind loads and responses were typically obtained using aeroelastic model tests. In these tests, the structural properties are modeled in an equivalent lumped mass system with scaled natural frequencies and matched mode shapes. Wind speeds are scaled based on modeling requirements and the damping ratio has to be realized as part of the physical modeling. Not only is the design and construction of the aeroelastic model expensive and time-consuming, changes in either the geometry or the dynamic properties of the building require a new study with a new design of the model. With the pace of the design and construction of present day tall buildings, aeroelastic modeling is often not a practical option.

*Corresponding author, Director, E-mail: ericho@blwtl.uwo.ca

^a Senior Associate, E-mail: unyong@gradientwind.com

^b Associate Director, E-mail: pcc@blwtl.uwo.ca

The force balance technique, developed in the 1980's (Tschanz 1982), is an efficient method to determine structural wind loads on tall buildings in a wind tunnel test and is now widely used by for example, Boggs and Peterka (1989), Irwin and Xie (1993), and many others. In this technique, a rigid model with scaled geometry is mounted to a force measurement device at its base. The model requires no detailed dynamic design other than the natural frequencies of the balance-model system be sufficiently high to avoid the scaled natural frequencies of the prototype. Aerodynamic wind forces, including shears and moments, are measured in the wind tunnel at the base of the force balance model without concern to the details of the dynamic properties. The aerodynamic information includes the mean and quasi-steady dynamic components of the wind forces, as well as the frequency content of the dynamic wind forces. These quantities are sufficient for the analysis of the wind tunnel data in order to provide two main pieces of information needed for the building design; namely, the acceleration response at the top of the building and the distributed design loads with height. This is possible due to the fact that the wind forces can be non-dimensionalized by the reference dynamic pressure and the building dimensions, and the frequency content can be scaled using the non-dimensional reduced frequency. The analysis for accelerations and subsequently the inertial loads is based on random vibration theory. From this theory the superposition of the modal responses is determined from the mechanical admittance of the building response function with dynamic amplification at the natural frequencies of the building.

The force balance method requires a number of inherent assumptions and has some limitations. In the sway directions, for which the model has a linear mode shape, the base moment can be converted to generalized forces without any knowledge of the load distribution with height. However, there is no obvious conversion from the measured base torque to the generalized force due to torsion. This is because the base torsion on the rigid force balance model is assembled with an inherent constant influence function on the distributed torsion over the building height, whereas most buildings have a more or less linear mode shape in the torsion direction. A number of algorithms have been developed by different groups to correct the effect of non-linear mode shape (Vickery *et al.* 1985, Holmes 1987, Xu *et al.* 1993, Xie and Irwin 1998, Holmes *et al.* 2003). The correction for slightly non-linear sway mode shapes is relatively simple and most methods are effective. The correction for generalized force due to torsion is not so straightforward. Corrections are applied as empirical factors, derived based on assumed load shapes.

Another inherent limitation in the force balance test technique is that it requires a monotonic variation of mode shape with height. This is not usually an issue for most tall buildings as the first fundamental mode in each of the three principal directions generally has a monotonic mode shape. Furthermore, at higher modes the first harmonics usually come with relatively high natural frequencies where there is not sufficient fluctuating energy in the natural wind to cause significant dynamic effects. For very tall or unusually flexible structures these higher modes can be influential.

Beyond the corrections due to non-linear mode shape to evaluate the generalized forces, a number of details in the analysis were omitted in the early days of using the force balance method. This includes the omission of all cross-directional terms in forming the generalized forces for coupled systems, as well as omitting the cross-modal terms in the superposition of the modal quantities to determine building responses. The empirical white noise approximation in estimating the area under the resonant peak is still widely used. There are also additional assumptions made in formulating a set of load combination factors for use in the design.

Generally, force balance wind tunnel data are analyzed in the frequency domain. This is carried over from the early days when computing power and storage capacity were limited. Wind tunnel measurements would be taken in the time domain but immediately processed to extract the basic data in the form of mean and fluctuating wind force statistics, and spectra of base overturning moments and torsion. The measured time series were then discarded in order to limit the storage requirement.

During the transition in the force balance technique from handling simple uncoupled buildings to the sophistication that allows analysis of all conceivable complexity, the effect of dynamic coupling became more critical but it was, at times, mishandled. With increasing power and storage capacity in computing systems, there was a natural progression to keep all the time series measurements, thereby allowing later analysis of the data including consideration of correlation and coupling effects.

With the availability of the wind force time series, it becomes more straightforward to carry out time domain analysis which can handle the correlation and coupling effects implicitly. Formulations of frequency and time domain analyses are presented in this paper.

A tested building is used as an example to briefly examine the effects of the various levels of simplifications in analyzing the wind tunnel force balance data. These effects are highly variable depending on the wind force correlation and dynamic properties. The example is intended for illustration and does not indicate ranges of errors. Variations and particular problems associated with testing are not discussed in this paper.

2. Components of force balance analysis

The analysis of the force balance data taken in the wind tunnel tests includes a number of steps where assumptions or simplifications are required. This section reviews the components and methodologies of the force balance analysis in historical perspective, and discusses the improvements that have been introduced to the process.

2.1 Coupled wind forces

Early uses of the force balance technique for buildings which were by today's standard relatively simple and small, often encountered dynamic properties that were uncoupled. Because of computing and storage limitations, only the statistics and auto-spectra of the base moments were recorded. Generally, to form the generalized forces contributions of the cross-coupling terms in the mode shapes were included in the calculation based on their directional contribution to each mode. The correlation of the directional wind forces was largely ignored. In the case where there was significant coupling of directional wind forces, aeroelastic modeling was used to confirm results from force balance tests.

For a majority of buildings, the coupling between the two sway forces is generally small. However, the same cannot be said for torsion or in cases where the surrounding obstructions significantly altered the wind flow patterns. The consideration of the correlation of wind forces, particularly in the case where there is significant dynamic coupling, becomes important. On-line weighted-summing of signals allows more accurate determination of the generalized forces without requiring storing of the time series of measurements. However, it is cumbersome in the case when the dynamic properties change.

With added storage capacity, the solution utilized currently is to store all time series of base shears and moments, thereby allowing post-processing of the base forces into estimates of the generalized forces. By assembling the time series of the generalized forces at each time increment, all inherent cross-correlation of wind forces and the effects of modal coupling are readily included.

2.2. Mode shape correction

Early in the application of the force balance technique, it was recognized that most buildings do not have perfectly linear mode shapes, although many shorter buildings prevalent at the time did have mode shapes that were very close to linear. As building heights increase, the error in estimating generalized forces from the base sway moments assuming linear mode shapes needs to be addressed. In addition, the fundamental difference in the torsion mode shapes and the influence function of the base torque requires a significant correction to the generalized force component generated from the torsion wind forces.

The correction to non-linear mode shapes for the uniform torque influence function requires knowledge or estimates of the wind force distribution. Approximate correction factors may be developed through power law representation of both the wind force distribution and the mode shape. In practice, mode shape corrections are critical for the evaluation of the resonant dynamic component of the responses, e.g., accelerations, and the effect of the non-linear mode shapes on the spectral quantities is the most critical. For sway directions, Vickery *et al.* (1985) provided a methodology to consider the spectral content using empirical wind properties. Vickery [undated] and Holmes (1987) provided mode shape correction factors for the spectral content based on broad and narrow band responses for torsion. A nominally conservative correction was chosen as an empirical value for general use at the BLWTL. Studies on the sensitivity of mode shape correction suggest that they tend to be small and most methods for correction in the sway modal directions are very similar. For torsion, although the magnitude of the mode shape correction is large, it typically receives much less attention since it is often not critical in the structural design.

2.3 Modal coupling

Because of storage requirements, early wind tunnel tests only retained statistics of the base moments and torque and typically disregarded any correlation of the directional wind forces. Also, the cross-modal terms could not be determined without the simultaneous time series or the cross spectra of the wind forces. Although it is usually expected that the cross-modal terms are small, there are occasions that their effects are shown to be significant (Yip and Flay 1995).

As computing power improved, cross-spectra of wind forces were being measured and used in the analysis. However, the re-construction of the directional responses would still routinely ignore the cross-modal terms. While it is generally true that the cross-modal terms are small, the assembly of the resultant responses, such as total stresses or total accelerations, can be done more accurately with additional information regarding the cross-modal effects. In the typical application of the white noise approximation of the resonant component, there is no mechanism to include the cross-modal terms when assembling the directional responses.

In the updated formulation, all cross-correlations in the directional forces are inherently included by evaluating generalized forces for each time increment. The calculation of the responses also includes all cross-modal terms and all resultant quantities can be determined accurately. The complete formulation is found in Section 4.

2.4 Complete quadratic combination

For the case where the natural frequencies in two adjacent modes are close, the use of the white noise approximation to estimate the resonant amplification becomes problematic because the interaction of the two resonant peaks at similar frequencies cannot be accounted for. As a simple illustration of this inadequacy, consider a square building with similar frequencies in its first two modes. The resultant accelerations are first derived from an analysis with an assumed orthogonal axis system normal to the building faces, resulting in highly coupled modes. The analysis is then repeated with a diagonal axis system which effectively eliminates the coupling. It was found that the results can be different by up to 40% when the resultant accelerations are determined from square-root-sum-of squares (SRSS) of the component accelerations without consideration to the effects of the similar modal frequencies. The interference of two sinusoidal series effectively reduces the single resonant peak in frequency domain into two smaller peaks at slightly different frequencies. This cannot be captured by the SRSS calculation of the component resonant responses derived from the analytical white noise approximation.

One suggested solution to this is the application of the complete quadratic combination (CQC) method (Der Kiureghian 1980). This method has been used extensively in the field of earthquake engineering. However, due to the source of seismic excitation by sinusoidal waves at the base, the forcing function in different axes of the building is highly coupled; whereas the coupling of aerodynamic wind forces is much more complex. Chen and Kareem (2005) suggested that the cross correlation of the wind forces should be considered in the calculation. The application of the modified CQC method shows that it can greatly reduce the differences observed from analyzing the two different axis systems, such as for the square building example above, and thus provide more rational results. Subsequent experience in applying this method suggests that for a majority of buildings the cross-modal effect is negligible; only in the case where the frequencies of the two modes are nearly identical do the cross-modal effect needs to be considered. Whereas the original CQC method suggests that a correction to the SSRS estimates may be required when there are differences in frequencies of up to 10%, the modified CQC with cross-modal wind components gives minimal correction when frequency differences are as small as 2%.

Nonetheless, the assembling of the resultant responses from the directional responses still requires consideration of the cross-modal terms to account for the non-simultaneous occurrence of these directional responses. The use of the complete coupled 3-D analysis eliminates the need for the CQC to determine combined peak quantities. The complete formulation in both time and frequency domain analyses can include these effects.

2.5 Resultant accelerations

Since structural loads are critical for the design of a building, conservative estimates of wind loads are generally accepted in the interest of safety. However, for the evaluation of accelerations, overly-conservative estimates may create an unnecessary alarming situation and delay in the overall progress of the building construction. It is widely acknowledged that the SRSS values of the directional peak responses are overly conservative because it assumes perfect correlation among directional components.

Two general methods have been applied to estimate the peak resultant acceleration from component peak accelerations. The first is known as the Joint Action Factor (JAF) (Isyumov 1993, 2002). This stems from the premise that the component peaks do not occur at the same time, and

the SRSS peak should be factored down from the upper bound SRSS resultant. An empirical formula has been developed based on mathematical limits and from aeroelastic model test results where the directional accelerations were measured and combined in real time. The joint action resultant from two contributing components is written

$$a_r = a_{\min} + 0.333(a_{\max} - a_{\min}) \quad (1)$$

where a_r is the resultant acceleration, a_{\max} and a_{\min} are the larger and smaller of the directional accelerations, respectively. The second method is the Coincident Action Factor (CAF) (Isyumov 1993, 2002). This is based on the idea that the peak resultant will most likely occur when one of the directional acceleration components is itself a peak value. The CAF is an empirical reduction factor based on a collection of data. It is applied to the smaller of the directional components which is then added to 100% of the larger of the directional components.

$$a_r = \sqrt{a_{\max}^2 + 0.5(a_{\min 1}^2 + a_{\min 2}^2)} \quad (2)$$

where a_{\max} is the largest of the directional accelerations and $a_{\min 1}$ and $a_{\min 2}$ are the remaining two directional accelerations. Note that $a_{\min 1}$ and $a_{\min 2}$, are interchangeable among the remaining load directions without affecting the results. Although it is more intuitive, this method does not work well for cases where the acceleration components are similar in magnitude and highly coupled. In that case, the reduction to the smaller directional component will be excessive.

2.6 Peak factor

The assembly of the peak responses from the mean and dynamic components requires the use of a peak factor. For engineering application, a conservative value of 3.8 has been adopted. Many building codes have now adopted the practice of using different peak factors for the background dynamic and the resonant dynamic components. The peak factor for the background component ranges between 3.7 in the Australian Standard (AS/NZS1170: 2011), and 3.4 in ASCE (2010), (*Note: the peak factor in the Australian Standard was revised to 3.4 in a later amendment*). The peak factor for the resonant component is evaluated using the cycling frequency of the process. From experience with low buildings or buildings immersed in highly turbulent environment, the peak factor for the background component can be much higher than 3.4. While this value may be appropriate for code use because of the conservative specification of the mean values, it may be un-conservative for use with the measured wind loads in the wind tunnel. For wind tunnel tests, the peak factor for the background component should be evaluated directly from the data and the peak factor for the resonant component evaluated using the cycling rate of the process.

2.7 Effective loads

Equivalent static load shapes are used in the structural design of tall buildings. Depending on the structural influence coefficients of the structural members in the building, the effective loads may have significantly different shapes. For tall buildings, the load shapes required to design the major structural members can generally be enveloped by the load shapes corresponding to the peak base shear and peak base moment. In force balance data analysis, the peak base moment has been

used as the default load response for the generation of effective load shapes for overall structural design. It should be noted that for special structures, other critical load effects may be used to generate additional critical load cases for design; for example, in the case of a structural link connecting multiple towers, the influence function of the structural link due to loads on the tower components may be more appropriate.

The basic outputs from the force balance test and analysis are the building responses; in particular, the accelerations at the uppermost habitable floor, and the base moments calculated by summing the contribution from the mean, the background dynamic and the inertial load components. For the purpose of carrying out structural design, however, the wind-induced loads distributed over the building height is required. While summing the loads to the base provides a good benchmark that the structural designers can use to compare with their preliminary design, the detailed design requires the mean and background base moments to be distributed over the height of the building and combined with the level-by-level inertial loads.

A number of schemes have been used over the years to estimate the mean and background load distribution over the building height. This includes assuming the mean component taking on the mean wind speed profile; both the mean and background components taking on the mean wind speed profile; or the background dynamic component following the inertial load shape. Each of these has its own shortcomings because the actual wind force profile on the building is highly variable in space and time. The load shapes will also differ by wind direction. It should be appreciated that the effective loads are a representation of the wind forces that will produce the targeted peak load effects. It is not intended to recreate critical load distributions at any time increment or specific wind direction. Acceptance of this is vital in allowing assumptions to derive equivalent static load distributions for structural design.

The current method at the BLWTL makes use of the measured base shear and base moment data to derive a more representative wind force profile relative to the actual measurements for different wind directions. For the quasi-steady load component, a trapezoidal load shape is developed that satisfies the measured quasi-steady shear and moment peak coefficients for each wind direction. For the inertial load component, the shape is proportional to the product of the story mass and mode shape; generally, the dominant mode shape for each direction is used as representative. For each wind direction, the relative contribution of the quasi-steady peak and the inertial load components are determined. The combined load shape is formed from linear combination of the quasi-steady and the inertial load shapes, weighted by their relative contributions.

In specifying distributed wind loads for overall structural design, it is generally not necessarily to consider load distributions for all wind directions. To minimize the number of load cases for design, some laboratories would specify load shapes derived for selected dominant wind directions to satisfy the predicted base moments and/or base shears. The method used at the BLWTL is to carry out weight-averaging of the load shapes from all wind directions based on the contribution of each direction to the overall prediction of the base moments. In this case, the contribution is defined as the relative count of the number of crossings* for different wind directions.

* The number of crossings is determined from the prediction process where the angle-by-angle wind effect variations, as a function of wind speed, are combined with a statistical wind climate model to predict exceedance of the load effect over a target return period. This process is not discussed in detail here. See Irwin *et al.* (2005) for further discussion.

2.8 Load combination factors

The determination of the directional wind loads using the force balance method produces the peak base moments and their corresponding equivalent static load distributions. For the design of the structure, using the peak loads in the x, y and torsion directions simultaneously would be conservative since these peaks occur at different times and also for different wind directions. Earlier attempts to develop load combination factors, for the purpose of rationally combining the loads in each of the x, y, and torsion directions, have utilized the joint action concept analogous to that previously described for resultant accelerations. Nominal load cases include the application of 100% of each of the wind loads in a single direction, the application of combinations of wind load in two directions with a factor of 0.8 or 0.85, and the application of positive and negative combinations of wind loads in the three directions with a factor of 0.7 or 0.75.

A more intuitive companion load concept is now widely used to derive load combination factors. This is based on the assumption that the worst load condition will likely occur when one of the directional wind loads is at its peak value. Also, at the time when the governing peak load is at 100%, there will be simultaneous occurrence of other directional wind loads, although not at their individual peak values. With all positive and negative combinations of x, y, and torsion loads, 24 load cases result. For each load case, one of the load components will be 100% of its peak in either the negative or positive direction.

Unlike resultant accelerations, the structural design of buildings is primarily targeted to stress level which is a linear combination of the influence of the directional wind loads. The method utilized at the BLWTL is based on the calculation of the target load effects generated by the directional wind loads. Defining the directional load effect as the product of the directional influence coefficient and the directional wind loads, pseudo influence coefficients reflecting the relative influence from x, y and torsion directions are used to calculate pseudo load effects for this exercise. Conceptually, the pseudo load effects are formulated to be the linear sum of the effects due to x, y and torsion loads. Instead of evaluating actual influence function of member stresses, the relative influence due to each of the directional loads is used. The general cases include equal influence coefficients among all three directions or equal load effects among the three directions. It was found that the results from these two sets of influence coefficients are similar and equal load effects are generally used to evaluate load combination factors. In the calculations of the load effects, all cross spectral properties are taking into account.

The combined load factors to be used with the predicted peak loads in each of the load directions have to be sufficient to produce the predicted load effects.

$$\hat{E} \leq c_x \gamma_x \hat{M}_x + c_y \gamma_y \hat{M}_y + c_t \gamma_t \hat{M}_t \quad (3)$$

where \hat{E} is the predicted load effect, c are the load combination factors and γ are the relative influence coefficients for the pseudo load effect considered.

From the wind force measurements determined from the force balance tests, peak load effects for all wind directions are determined for several cases; using all three directional wind loads and using combinations of two directional wind loads. These load effects are then combined with the wind climate model to determine predicted load effects for the corresponding return period. By first considering the predicted load effects from using two directional loads, and using 100% of the peak load in one of the directions as the primarily load direction, the load factor for the secondary load direction can be determined. Repeating this process for all combinations gives 12 different

combinations. For all these cases, the combinations are then further checked against the predicted load effects by using all three directional loads to arrive at the last tertiary load factors in both positive and negative signs, giving a total of 24 load cases. The results from this process are usually very close to the general companion load factor of 0.4 to 0.6 using simple assumptions, but it has inherently taken into account the potentially different levels of correlation among different wind load directions.

3. Extended applications of the force balance technique

Since the development of the force balance technique, not only are the buildings getting taller to challenge the basic idea of linear mode shapes, the building geometry has steadily become more complex. Common cases of complexity include buildings with significant changes in their geometry along the building height and building groups with common lower levels. There are other complexities but the above two cases will be briefly discussed here.

3.1 Buildings with significant change in geometry

With architectural design being progressively more innovative, there are often unique changes in building forms within the same building. One fundamental change in building form is the extensive use of large podiums. The other is cutbacks in the geometry at upper floors. Since the force balance is taking aerodynamic wind force and moment measurements at a single point at the base of the model, the analysis is generally carried out at the same coordinates along a vertical axis of the building. Inertial loads are calculated using first principles at the centers of masses. They are converted to the center of analysis and added to the aerodynamic wind loads to obtain the peak loads. For buildings with significant cutbacks, the distribution of the wind loads becomes more uncertain even though the base forces and moments are correctly measured. While this does not affect the sway loads, it does have a large impact on torsion.

Recall that the accumulation of torsion at the base of the building is based on a constant influence coefficient along the height of the building, whereas the generalized force due to torsion is weighted by the mode shape. Assumptions were being made and empirical correction factors derived based on a simple representation of distributed torsion and mode shape along the height of the building. With significant offset or changes in the basic form, there arises the possibility of a much different torsion shape than assumed. This can affect the estimate of the generalized forces due to torsion. No systematic study has been done to clarify this situation due to the fact that the potential variations are endless.

Assuming that a reasonable generalized force can be obtained due to torsion and the force balance analysis can proceed, additional difficulty is encountered when faced with the prospect of distributing the torsion design loads over the building height. The main difficulty lies in the fact that the mean torsion may be positive or negative and the dynamic component is cycling about the mean but is generally treated as a positive value. In the case where the torsion changes sign along the building height, the dynamic component may reduce the overall design loads if not handled properly. General schemes to estimate the effect of geometric offset using general geometric eccentricities are used to provide a more realistic relative distribution of torsion over the height of the building. This generally produces a kink in the distributed mean torsion.

Two techniques have been used to eliminate under-specification of torsion design loads. One is

to calculate the dynamic component following the same sign of the mean. This will ensure that the total peak magnitude is correct. When the effective loads are applied in positive and negative directions, peak torsion will be enveloped.

In some cases, when the cutback is over a significant portion of the building, the procedure mentioned above can be significantly conservative. In that case, a second technique is used where the building is analyzed at two different centers, one corresponding to the center of the upper portion of the building and the other corresponding to the overall building footprint. The specification of the design torsion is determined in two steps. For the upper portion, the distributed torsion is determined using the analysis using the upper center. For the lower portion, the accumulated loads from the upper portion are specified as point loads (in x, y and torsion directions) at the transfer point, together with the distributed wind loads derived from the analysis using the lower center.

3.2 Multi-component system

Increasingly, large developments include multiple towers, often with a large podium at the base. Depending on the design, the towers and the podium may be structurally connected with cross-coupling responses amongst the towers. As long as the structural dynamic analysis is carried out based on a connected system, the coupling characteristics will be apparent in the resulting mode shapes and natural frequencies. For such connected system, a multi-balance technique is used to derive the generalized forces from each component in the system.

A multi-balance rig has been designed at the BLWTL to accommodate multiple balances. The tower models are mounted on the balances separately and the base shear and base moment measurements taken simultaneously but independently. Low podiums are typically ignored in the tower model as they contribute little to the generalized forces. However, multi-level podiums with significant heights are sometimes treated as part of the towers. The aerodynamic data for each tower are then converted to generalized forces using the usual technique. The contributions from all component towers are summed to form a time series of system generalized forces for each mode. Dynamic coupling seen in the mode shapes dictates the number of modes to be used in the analysis, but all fundamental x, y and torsion modes for each tower should be included. This may mean nine (9) modes or less for a three (3) tower system, for example.

Once the generalized forces have been determined, the analysis proceeds for each tower independently for the determination of accelerations and distributed wind loads for the superstructure. Assembly of the inertial loads makes use of the mode shapes from the individual towers.

In addition, for the design of the foundation, the overall quasi-steady wind forces for the entire system are determined by summing the forces taken for the individual towers. This inherently includes the effects of correlation of the forces among different components. The overall generalized forces determined from the individual components are also valid for the overall system. The system is then analyzed using the normal procedure to determine the overall base moments for the foundation. For the inertial load component, contributions from all components are summed. This removes the conservatism of applying the peak loads from all individual towers.

For structural design, two sets of effective loads are given. One set is for the design of the tower structures where the independent peak loads on each tower are provided. The other set is for the podium or foundation level where the specified peak loads for the towers may be used with a reduction factor to account for the non-simultaneous occurrence of peak wind loads on the

components.

The details of structural transfer among the component towers are not required since the quasi-steady wind loads are based entirely on the aerodynamic characteristics and the inertial loads are based on the response characteristics and the mass of the towers. The relative responses in the component towers are included through the use of the coupled mode shapes. The load transfer will occur in the structural analysis program once these wind loads are applied onto the structure.

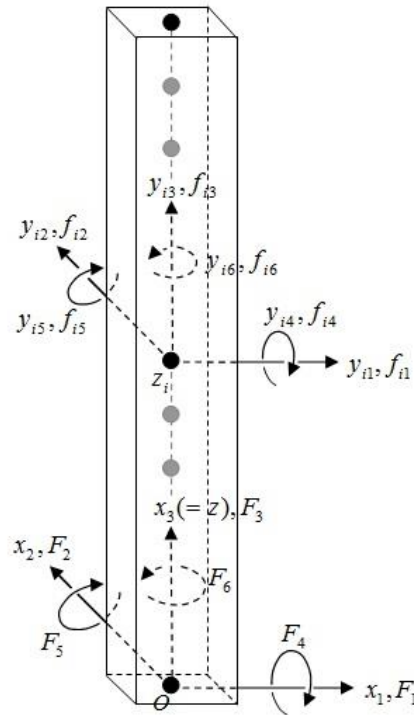


Fig. 1 Building structure and definition of forces and displacements

4. Governing equations for dynamic wind loads and responses

The force balance technique is applied to line-like structures fixed at the base. The dynamic properties of the line-like structure are represented by a distributed mass system along its height with associated mode shapes in the x and y sway and torsion directions. Fig. 1 shows the definition of coordinate of a 6 degree of freedom system, to define the displacements, \mathbf{y} , forces, \mathbf{f} , and base moments \mathbf{F} in discrete form. These vectors can be presented as follows

$$\mathbf{y} = \{\mathbf{y}_1^T, \mathbf{y}_2^T, \dots, \mathbf{y}_6^T\}^T \quad (4)$$

$$\mathbf{f} = \{\mathbf{f}_1^T, \mathbf{f}_2^T, \dots, \mathbf{f}_6^T\}^T \quad (5)$$

$$\mathbf{F} = \{F_1, F_2, \dots, F_6\}^T \quad (6)$$

By definition, the base moment

$$\mathbf{F} = \mathbf{N}\mathbf{f} \quad (7)$$

where

$$\mathbf{N} = \begin{bmatrix} \mathbf{u}^T & \mathbf{0} & \mathbf{0} & \mathbf{0} & \mathbf{0} & \mathbf{0} \\ \mathbf{0} & \mathbf{u}^T & \mathbf{0} & \mathbf{0} & \mathbf{0} & \mathbf{0} \\ \mathbf{0} & \mathbf{0} & \mathbf{u}^T & \mathbf{0} & \mathbf{0} & \mathbf{0} \\ \mathbf{0} & -\mathbf{z}^T & \mathbf{0} & \mathbf{0} & \mathbf{0} & \mathbf{0} \\ \mathbf{z}^T & \mathbf{0} & \mathbf{0} & \mathbf{0} & \mathbf{0} & \mathbf{0} \\ \mathbf{0} & \mathbf{0} & \mathbf{0} & \mathbf{0} & \mathbf{0} & \mathbf{u}^T \end{bmatrix} \quad (8)$$

In Eq. (8) above, elevation vector $\mathbf{z} = \{z_1, z_2, \dots, z_l\}^T$; $\mathbf{u} = l$ -dimensional vector of ones; $\mathbf{0} =$ vector of zeros; l is the number of lumped masses in the system.

In the force balance test, the distributed wind forces on the model are measured as five component forces at the base. The system in the Fig. 1 shows the measured base forces; namely, two shear forces of F_1, F_2 for x_1 and x_2 -directions and two bending moments of F_4, F_5 and a torque, F_6 . F_3 is not measured because it is generally ignored for vertically distributed structures.

In the case of a linear mode shape (refer Fig. 2), the generalized modal forces for sway forces can be evaluated without knowing the wind load distribution. In the case of torsion, there is no general relationship between base torque and generalized torque due to the significant difference between the fundamental torsion mode shapes (generally linear from zero at the bottom to a maximum at the top) and the influence function of distributed torsion to base torsion (uniform function with height). Investigation of the relationship between the generalized torque and base torque through a range of load shape and mode shape functions suggests that the generalized torque may be approximated conservatively by 0.7 x base torsion. The modal matrix becomes

$$\mathbf{q}_F \cong \begin{bmatrix} a_{11}\mathbf{z}/H & a_{12}\mathbf{z}/H & \dots & a_{1n}\mathbf{z}/H \\ a_{21}\mathbf{z}/H & a_{22}\mathbf{z}/H & \dots & a_{2n}\mathbf{z}/H \\ \mathbf{0} & \mathbf{0} & \dots & \mathbf{0} \\ \mathbf{0} & \mathbf{0} & \dots & \mathbf{0} \\ \mathbf{0} & \mathbf{0} & \dots & \mathbf{0} \\ 0.7a_{61}\mathbf{u} & 0.7a_{62}\mathbf{u} & \dots & 0.7a_{6n}\mathbf{u} \end{bmatrix} \quad (9)$$

In the above, a_{ik} = maximum amplitude of the mode at the top of the building to the direction i ($= 1$ to 6) of mode k ($= 1$ to n). The modal load vector in (5) can be approximated as follows

$$\tilde{\mathbf{f}} \cong \mathbf{q}_F^T \mathbf{f}. \quad (10)$$

For the torsion direction, an empirical conversion from constant influence coefficient for base torsion to linear mode shape is used, as discussed in Section 2.2.

In expanded form, it can be written

$$\tilde{\mathbf{f}} \cong \begin{Bmatrix} \frac{a_{11}}{H} \mathbf{z}^T \mathbf{f}_1 + \frac{a_{21}}{H} \mathbf{z}^T \mathbf{f}_2 + 0.7a_{61} \mathbf{u}^T \mathbf{f}_6 \\ \frac{a_{12}}{H} \mathbf{z}^T \mathbf{f}_1 + \frac{a_{22}}{H} \mathbf{z}^T \mathbf{f}_2 + 0.7a_{62} \mathbf{u}^T \mathbf{f}_6 \\ \vdots \\ \frac{a_{1n}}{H} \mathbf{z}^T \mathbf{f}_1 + \frac{a_{2n}}{H} \mathbf{z}^T \mathbf{f}_2 + 0.7a_{6n} \mathbf{u}^T \mathbf{f}_6 \end{Bmatrix} \quad (11)$$

Following the definition of base moments (F_4, F_5, F_6)

$$F_4 = -\mathbf{z}^T \mathbf{f}_2 \quad (12)$$

$$F_5 = \mathbf{z}^T \mathbf{f}_1 \quad (13)$$

$$F_6 = \mathbf{u}^T \mathbf{f}_6 \quad (14)$$

Eq. (10) becomes

$$\tilde{\mathbf{f}} \cong \begin{Bmatrix} \frac{a_{11}}{H} F_5 - \frac{a_{21}}{H} F_4 + 0.7a_{61} F_6 \\ \frac{a_{12}}{H} F_5 - \frac{a_{22}}{H} F_4 + 0.7a_{62} F_6 \\ \vdots \\ \frac{a_{1n}}{H} F_5 - \frac{a_{2n}}{H} F_4 + 0.7a_{6n} F_6 \end{Bmatrix} \quad (15)$$

The generalized forces in (15) can expressed as linear functions of base forces

$$\tilde{\mathbf{f}} \cong \mathbf{q}_B \mathbf{F} \quad (16)$$

where

$$\mathbf{q}_B = \begin{bmatrix} 0 & 0 & 0 & -\frac{a_{21}}{H} & \frac{a_{11}}{H} & 0.7a_{61} \\ 0 & 0 & 0 & -\frac{a_{22}}{H} & \frac{a_{12}}{H} & 0.7a_{62} \\ \vdots & \vdots & \vdots & \vdots & \vdots & \vdots \\ 0 & 0 & 0 & -\frac{a_{2n}}{H} & \frac{a_{1n}}{H} & 0.7a_{6n} \end{bmatrix} \quad (17)$$

Finally, the modal dynamic equation in generalized coordinates can be expressed as the following governing equation

$$\tilde{\mathbf{M}} \ddot{\tilde{\mathbf{y}}} + \tilde{\mathbf{C}} \dot{\tilde{\mathbf{y}}} + \tilde{\mathbf{K}} \tilde{\mathbf{y}} = \tilde{\mathbf{f}} \quad (18)$$

In the above, $\tilde{\mathbf{M}}, \tilde{\mathbf{C}}, \tilde{\mathbf{K}}$ = modal mass, damping, stiffness matrices of the structure, respectively, and are all diagonal matrices; the dot and double dot over the variables represent the first and second order time derivatives.

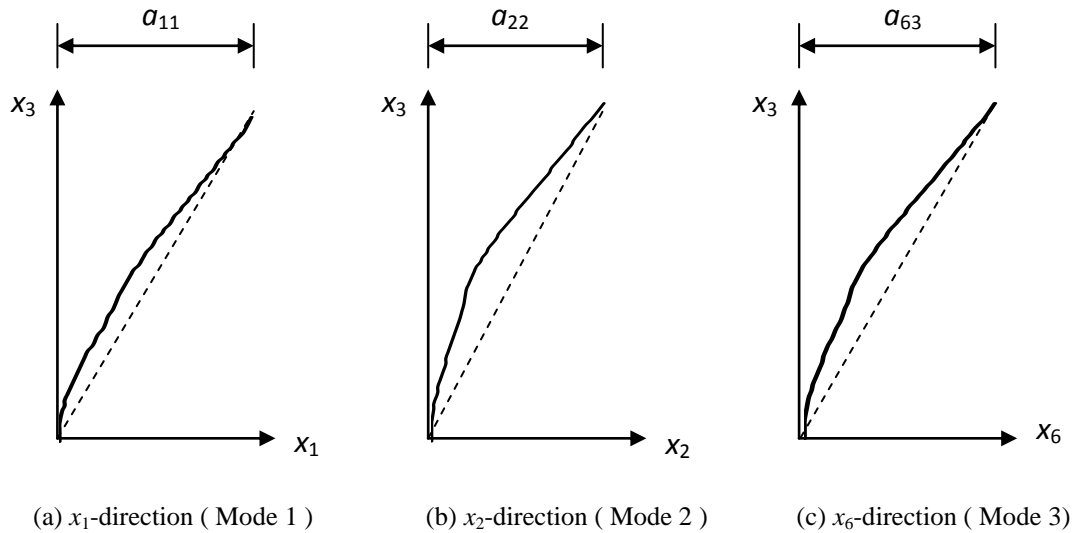


Fig. 2 An example of the assumed linear mode shapes for force balance analysis

5. Analysis of the wind tunnel force balance data

5.1 Frequency domain analysis

Earlier studies using the force balance method have utilized an empirical formula to evaluate the resonant component, whereas the background component is taken from the wind tunnel aerodynamic data. That also carried the inherent assumption that the cross-modal effect can be ignored. It has been shown that this assumption is not necessarily valid for all cases (Yip and Flay 1995) and there is a need to consider resonant on all modal forces including the cross-modal terms. The use of the empirical formula to evaluate the resonant responses introduces significant difficulties when it needs to include the cross spectra of the modal forces among different modes in the off-diagonal terms of the spectral modal forces (Eq. (19)) when considering the coupled modal force effect. Furthermore, it is not possible to implement additional frequency-dependent parameters such as aerodynamic damping and stiffness. Using the time series of generalized forces as presented in the previous section, calculations of all cross-spectral terms can be made in the frequency domain.

The complete set of cross-spectral modal forces, $S_{\tilde{\mathbf{f}}}$, is expressed in the following form

$$S_{\tilde{\mathbf{y}}} = \tilde{\mathbf{H}}^* S_{\tilde{\mathbf{f}}} \tilde{\mathbf{H}}^T \quad (19)$$

$$S_{\dot{y}} = \omega^2 S_y \quad (20)$$

$$S_{\ddot{y}} = \omega^4 S_y \quad (21)$$

where $\tilde{\mathbf{H}} = (-\omega^2 \tilde{\mathbf{M}} + j\omega \tilde{\mathbf{C}} + \tilde{\mathbf{K}})^{-1}$ is the complex mechanical admittance function; $j = \sqrt{-1}$. S_y is the spectrum of the generalized response, $S_{\dot{y}}$ is the spectrum of the generalized velocity and $S_{\ddot{y}}$ is the spectrum of the generalized acceleration. The covariance matrices of the generalized coordinate and its time derivatives, $\sigma_y^2, \sigma_{\dot{y}}^2, \sigma_{\ddot{y}}^2$ can also be calculated by the direct integration over the frequency domain as mentioned in the above paragraph

$$\sigma_y^2 = \int_0^{\infty} S_y df \quad (22)$$

$$\sigma_{\dot{y}}^2 = \int_0^{\infty} S_{\dot{y}} df \quad (23)$$

$$\sigma_{\ddot{y}}^2 = \int_0^{\infty} S_{\ddot{y}} df \quad (24)$$

It is commonly known that integrating in the frequency domain results in an inaccurate solution unless it has a very fine frequency resolution. However, doing so will lead to computational inefficiencies. To reduce the computation time, non-uniformly distributed frequency steps are used for the frequency domain integration. The increments around the modal frequencies are set to be much more refined than much of the remaining frequency domain. As well, more refined frequency intervals are used in lower frequency ranges to get improved results of the background component. Further details are not presented on this topic as it is not within the scope of this paper, the overall computation time is drastically reduced to the practical range.

With the complete set of cross-modal terms available, the variance of sway and torsion responses ($y_1, y_2, y_6, \dot{y}_1, \dot{y}_2, \dot{y}_6, \ddot{y}_1, \ddot{y}_2, \ddot{y}_6$) at any point (x_1, x_2) of the building can be determined as follows

$$Var(y_1, y_2, y_6) = diag(\mathbf{TQ}\sigma_y^2\mathbf{Q}^T\mathbf{T}^T) \quad (25)$$

$$Var(\dot{y}_1, \dot{y}_2, \dot{y}_6) = diag(\mathbf{TQ}\sigma_{\dot{y}}^2\mathbf{Q}^T\mathbf{T}^T) \quad (26)$$

$$Var(\ddot{y}_1, \ddot{y}_2, \ddot{y}_6) = diag(\mathbf{TQ}\sigma_{\ddot{y}}^2\mathbf{Q}^T\mathbf{T}^T) \quad (27)$$

$$\mathbf{T} = \begin{bmatrix} 1 & 0 & -x_2 \\ 0 & 1 & x_1 \\ 0 & 0 & 1 \end{bmatrix} \quad (28)$$

$$\mathbf{Q} = \begin{bmatrix} q_{c11} & q_{c12} & \cdots & q_{c1n} \\ q_{c21} & q_{c22} & \cdots & q_{c2n} \\ q_{c61} & q_{c62} & \cdots & q_{c6n} \end{bmatrix} \quad (29)$$

In the above, the matrix \mathbf{T} transforms the displacements at the center to those at another point; the subscript index c indicates that the values are defined at elevation z_c ; q_{c11} denotes the mode shape to the x_1 -direction of mode 1 at $z = z_c$; the other matrix components are defined in the similar way.

Total peak wind loads are evaluated from the total of the measured quasi-steady wind loads with the dynamic inertial load component derived from the responses as shown below.

$$\sigma_{\mathbf{F}_r} = \mathbf{NMq}\sigma_{\tilde{\mathbf{y}}} \quad (30)$$

Peak wind loads are assembled from the quasi-steady peak, including mean and background components, and the inertial load component.

$$\hat{F}_{it} = \bar{F}_i + \sqrt{g_{iq}^2 \sigma_{F_{iq}}^2 + g_{ir}^2 \sigma_{F_{ir}}^2} \quad (31)$$

for $i = 1$ to 6 base forces where g_{iq} is the peak factor for the quasi-steady base force/moment i and can be evaluated directly from the wind tunnel measurements. g_{ir} is the peak factor for the resonant component of base force/moment i and may be evaluated using the spectra of the corresponding resonant component forces.

$$g_{ir} = \sqrt{2 \ln(v_i T)} + \frac{0.577}{\sqrt{2 \ln(v_i T)}} \quad (32)$$

and

$$v_i = \left(\frac{\int f^2 S_{F_{ir}}(f) df}{\int S_{F_{ir}}(f) df} \right)^{1/2} \quad (33)$$

For lightly coupled and lightly damped system, v should approximate the natural frequency of the process.

5.2 Time domain analysis

Time domain analysis can be performed by the time integration of Eq. (18) for the given modal wind force time series $\tilde{\mathbf{f}}(t)$ and predefined (or assumed) initial condition. A state-space formula described below may also be used in the time domain analysis

$$\dot{\mathbf{X}} = \mathbf{A}\mathbf{X} + \mathbf{B}\tilde{\mathbf{f}} \quad (34)$$

$$\mathbf{y}_d = \mathbf{C}\mathbf{X} + \mathbf{D}\tilde{\mathbf{f}} \quad (35)$$

where

$$\mathbf{X} = \{\tilde{\mathbf{y}}^T, \ddot{\tilde{\mathbf{y}}}^T\}^T \quad (36)$$

$$\mathbf{A} = \begin{bmatrix} \mathbf{0} & \mathbf{I} \\ -\tilde{\mathbf{M}}^{-1}\tilde{\mathbf{K}} & -\tilde{\mathbf{M}}^{-1}\tilde{\mathbf{C}} \end{bmatrix} \quad (37)$$

$$\mathbf{B} = \begin{bmatrix} \mathbf{0} \\ \tilde{\mathbf{M}}^{-1} \end{bmatrix} \quad (38)$$

In (35), the desired response, for example, $\mathbf{y}_d = \{y_1, y_2, y_6, \dot{y}_1, \dot{y}_2, \dot{y}_6, \ddot{y}_1, \ddot{y}_2, \ddot{y}_6\}^T$ at location (x_1, y_1, z_c) can be acquired by using the following matrices

$$\mathbf{C} = \begin{bmatrix} \mathbf{TQ} & \mathbf{0} \\ \mathbf{0} & \mathbf{TQ} \\ -\mathbf{TQ}\tilde{\mathbf{M}}^{-1}\tilde{\mathbf{K}} & -\mathbf{TQ}\tilde{\mathbf{M}}^{-1}\tilde{\mathbf{C}} \end{bmatrix} \quad (39)$$

$$\mathbf{D} = \begin{bmatrix} \mathbf{0} \\ \mathbf{0} \\ \mathbf{TQ}\tilde{\mathbf{M}}^{-1} \end{bmatrix} \quad (40)$$

In the time domain analysis, the total force \mathbf{f}_t on the structure due to the dynamic motion can be calculated as follows by adding the inertial load \mathbf{f}_r together with the quasi-static load \mathbf{f} :

$$\mathbf{f}_t = \mathbf{f}_r + \mathbf{f} \quad (41)$$

where

$$\mathbf{f}_r = -\mathbf{M}\mathbf{q}\ddot{\tilde{\mathbf{y}}} \quad (42)$$

Therefore, using influence function matrix \mathbf{N} , the total base moments can be as follows

$$\mathbf{F}_t = -\mathbf{N}\mathbf{M}\mathbf{q}\ddot{\tilde{\mathbf{y}}} + \mathbf{N}\mathbf{f} \quad (43)$$

To calculate the resonant base forces \mathbf{F}_r using the time domain analysis, the \mathbf{C} and \mathbf{D} matrices (39) and (40), in the above section are modified as follows

$$\mathbf{y}_d = \mathbf{C}\mathbf{X} + \mathbf{D}\tilde{\mathbf{f}} \quad (44)$$

$$\mathbf{C} = \begin{bmatrix} \mathbf{TQ} & \mathbf{0} \\ \mathbf{0} & \mathbf{TQ} \\ -\mathbf{TQ}\tilde{\mathbf{M}}^{-1}\tilde{\mathbf{K}} & -\mathbf{TQ}\tilde{\mathbf{M}}^{-1}\tilde{\mathbf{C}} \\ \mathbf{N}\mathbf{M}\mathbf{q}\tilde{\mathbf{M}}^{-1}\tilde{\mathbf{K}} & \mathbf{N}\mathbf{M}\mathbf{q}\tilde{\mathbf{M}}^{-1}\tilde{\mathbf{C}} \end{bmatrix} \quad (45)$$

$$\mathbf{D} = \begin{bmatrix} \mathbf{0} \\ \mathbf{0} \\ \mathbf{TQM}^{-1} \\ -\mathbf{NMqM}^{-1} \end{bmatrix} \quad (46)$$

$$\mathbf{y}_d = \{y_1, y_2, y_6, \dot{y}_1, \dot{y}_2, \dot{y}_6, \ddot{y}_1, \ddot{y}_2, \ddot{y}_6, F_{1r}, F_{2r}, \dots, F_{6r}\}^T \quad (47)$$

where the resonant base shears and moments are $\mathbf{F}_r = \{F_{1r}, F_{2r}, \dots, F_{6r}\}^T$.

The instantaneous total base forces can be achieved by adding the above inertial loads with the quasistatic loads. The maximum and minimum dynamic peak base forces ($\max(\mathbf{F}_t)$, $\min(\mathbf{F}_t)$) can be estimated by using appropriate statistical method such as the Lieblein Method (Lieblien 1974).

5.3 Effective loads

The development of the effective load distributions with height from force balance analysis requires assumed load shapes for the mean and quasi-steady dynamic component and the inertial load components, the relative contribution of the mean, quasi-steady and inertial load components for the critical wind directions, the peak factor and in some cases, the relative contribution to the predicted base moment from different wind directions. For each wind direction, for directional load j

$$\mathbf{f}'_j = w_{jq}\boldsymbol{\Psi}_{jq} + w_{jr}\boldsymbol{\Psi}_{jr} \quad (48)$$

where \mathbf{f}' is the equivalent static load vector, w is the weighting factors for the quasi-steady peak and inertial load components and $\boldsymbol{\Psi}$ are the vectors of estimated load shapes.

The assumed load shapes are relatively straightforward as was discussed in Section 2.7. While the quasi-steady peak load distributions may be in the form of a trapezoidal load shape estimated from the base shear and base moment, the inertial load shape for each of the directional loads can be estimated from the uncoupled mode shape in the corresponding direction of the dominant mode.

In the frequency domain analysis described above, the dynamic responses were not evaluated independently. The relative contribution of the mean plus quasi-steady component and the inertial load component can be determined from the difference between the final peak moments and the quasi-steady peak moments from the wind tunnel measurements. This assembly of the peak moment in the frequency domain analysis requires a determination of the peak factor as discussed in Section 5.1.

Following Eq. (31) for the evaluation of the total wind loads, the relative contribution of the quasi-steady peak and the inertial load component can be written.

$$\mathbf{f}'_j = \left(\bar{F}_j + \frac{g_{jq}\sigma_{F_{jq}}}{\sqrt{g_{jq}^2\sigma_{F_{jq}}^2 + g_{jr}^2\sigma_{F_{jr}}^2}} \right) \boldsymbol{\Psi}_{jq} + \left(\frac{g_{jr}\sigma_{F_{jr}}}{\sqrt{g_{jq}^2\sigma_{F_{jq}}^2 + g_{jr}^2\sigma_{F_{jr}}^2}} \right) \boldsymbol{\Psi}_{jr} \quad (49)$$

The first of the two terms on the right side of the equation is the quasi-steady component while

the other term is the resonant component. Ψ is the estimated load shape normalized to unit base moment.

In the time domain analysis, the relative contributions of the quasi-steady peak and resonant components can be made where peak values can be obtained from respective time series of the measured and the total wind loads. There is no need to evaluate the peak factor as long as both the quasi-steady and the total peaks are adjusted to reference hourly values.

If desired, overall effective loads may be determined from weight-averaging of the contribution from different wind directions. This has been discussed in Section 2.7.

In wind tunnel test programs, the force balance test often precedes the local cladding pressure test. In that case, the equivalent static load distribution may later be updated using the integrated pressure data to obtain better estimates of the quasi-steady load shapes.

5.4 Contributions from modal components

Although not strictly required in the evaluation of the wind loads and responses, the relative contribution of the total dynamic wind loads from the background and resonant components from each mode is very useful in understanding the dynamic responses, and can be used as a basis for recommending mitigation; e.g., in the case of excessive dynamic responses. In using earlier analysis methods, this was straightforward with the peaks derived from the SRSS of all dynamic components. Due to modal coupling, the resonant force from each mode cannot easily be evaluated separately, either in the frequency domain or the time domain analyses described above.

One of two methods may be used to approximate the contribution of the resonant component from each mode. The first is to evaluate the resonant response due to each mode by ignoring the modal coupling effect, i.e., by deleting the off-diagonal terms in the covariance matrix of modal accelerations. The other approximation is possible by evaluating the incremental effect of each mode by sequentially including additional modes in the calculations. Firstly, the variance of the resonant force accumulated from mode 1 to k, $\text{var}(\mathbf{F}_{kr})$ can be calculated as

$$\text{var}(\mathbf{F}_{kr}) = \text{diag}(\mathbf{NM}\mathbf{q}_{(1-k)}\sigma_{\ddot{\mathbf{y}}_{(1-k)}}^2 \mathbf{q}_{(1-k)}^T \mathbf{M}^T \mathbf{N}^T), \text{ for } k = 1 \text{ to } n \quad (50)$$

Then, the accumulated total dynamic force can be expressed as follows

$$\hat{F}_{kt} = \sqrt{g_r^2 \sum_k \sigma_{F_{kr}}^2 + g_q^2 \sigma_{F_q}^2}, \text{ for } k = 1 \text{ to } n \quad (51)$$

The difference between the accumulated forces ($\hat{F}_{kt} - \hat{F}_{(k-1)t}$) can represent the contribution of mode i . This will in fact skew the effects towards those modes being evaluated first and care should be taken to include the dominant modes first.

6. Effects of analysis simplifications – an example case study

While Eq. (19) to (33) represent the complete solution, simplifications have been used in calculating the fluctuating responses. One simplification is the use of only the diagonal terms in the spectral force matrix. The other is the substitution of the mechanical admittance functions in

the formula by estimating the resonance responses using white noise approximation. Using an example building, the effects of using these simplifications are illustrated. For ease of comparison, wind tunnel data from a pressure test were used. The force balance analysis was carried out using base forces determined from integrating the local pressure data with corresponding tributary areas. The use of these data allows the comparison of the generalized forces derived from base moments with the mode shape correction algorithm to the more accurate values from integration of the wind forces with the mode shapes. With the paper aiming to compare the analysis methods, the use of one consistent set of data eliminates the uncertainties regarding the difference in the quality of data from the two test methods.

The building is a 154 m tall building with a simple 32 m by 54 m rectangular plan form and a large podium extending out to one side of the building. All analyses were carried out based on a center of coordinates at the center of the tower portion. The large but low podium does not contribute significantly to the generalized forces. Modal displacement is uncoupled in the x direction in the first mode, but coupled y and torsion directions in both the second and the third modes. The mode shapes are slightly non-linear. The natural periods are 8.6, 7.1 and 6.9 seconds for the first three modes, with the second and third mode periods quite close to each other. The building dimensions are typical but the building is soft relative to its size. It was tested in the simulated city environment with a tall building cluster to the northeast quadrant but fairly typical suburban exposure for the other wind directions.

The same data set was also analyzed using time domain analysis for validation purposes. In summary, the following analyses were carried out for comparison:

- A. Force balance data – simplified formulation using white noise approximation
- B. Force balance data – omitting cross-spectral terms, spectral integration
- C. Force balance data – complete coupled 3-D analysis
- D. Force balance data – time domain analysis

Analysis A represents the results obtained from commonly used simplified formulation in the evaluation of the resonant dynamic responses. For the calculation of the quasi-steady responses, the quasi-steady generalized forces may be used but the analysis is limited usually to the first 3 modes. The total quasi-steady responses through modal superposition are incomplete using only these few modes and the results would be unreliable. For the calculation of the accelerations, it is argued that the resonant peak dominates the contribution of the variance and the background component can be ignored. The variance due to resonance response is estimated by the area under the resonant peak. By using this simplified formulation, it has also ignored the cross modal terms outlined in the complete analysis.

Analysis B also omits the cross-spectral term in the generalized force matrix; e.g., in (19).

However, the evaluation of the variance is through integration of the displacement and acceleration spectra. Comparison between (A) and (B) therefore shows the difference in the calculation of the variance.

Fig. 3 shows analysis results from (A), (B), (C) and (D) listed above, based on the force balance methodology. In all cases, results for the uncoupled x mode agree very well, suggesting that the general simplified method is adequate when considering simple, uncoupled dynamic systems. By comparing results (C) and (D), it is seen that the full 3-D frequency domain analysis is complete, giving consistent results to the time domain analysis. The small differences between the two analyses are likely due to the less than ideal time resolution in the data set available for this investigation. Additional test and analysis are planned to further investigate this effect.

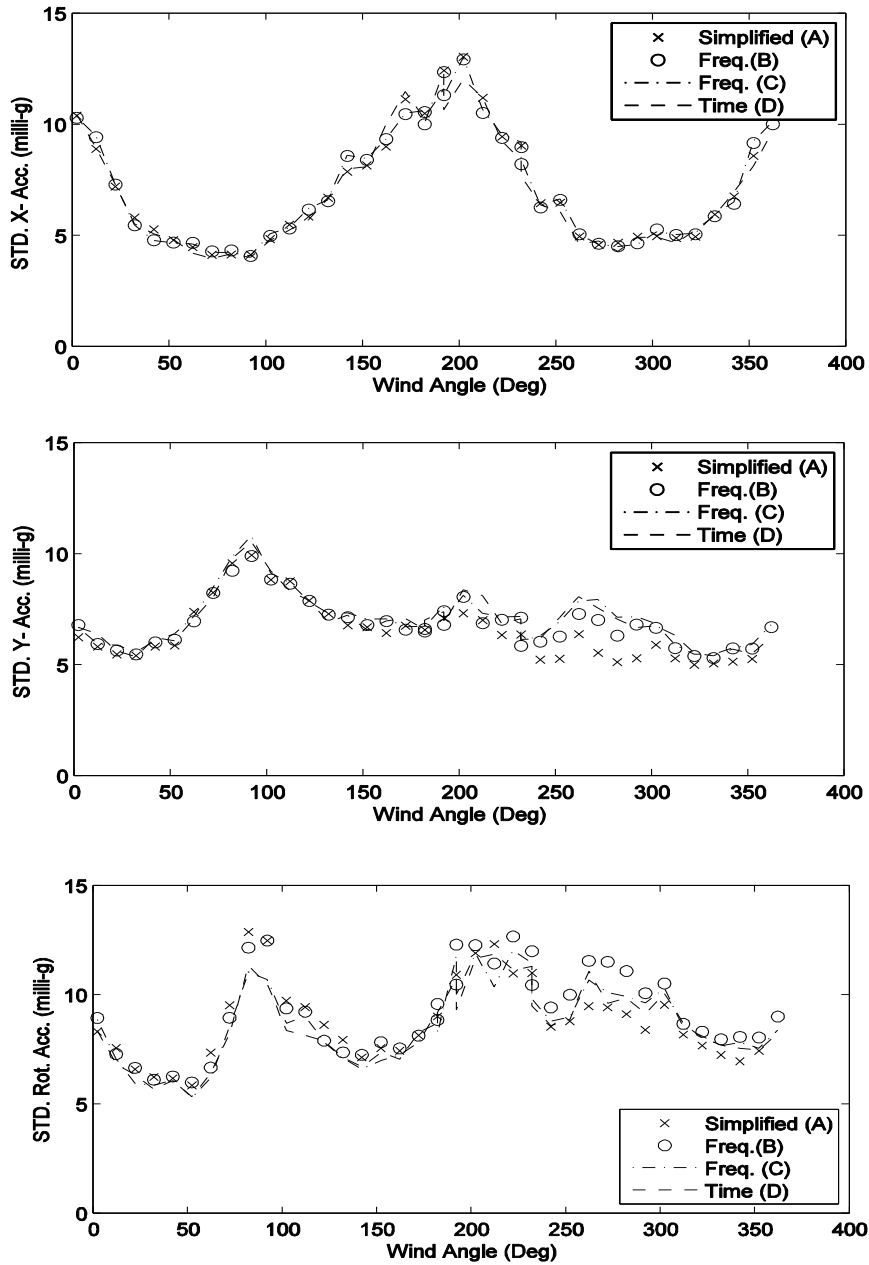


Fig. 3 Effects of simplified analysis procedures using force balance data

For the y and torsion responses, the effect of using the simplified formulae to calculate the variance is shown in the comparison between (A) and (B). Since the periods for the coupled second and third modes are quite close to each other, the simple estimate of the area under the resonant peak can be significantly different from results using integration of the spectral responses. Analysis (A) also included the complete quadratic combination (CQC) procedure which is found to modify the SRSS results by up to about 8%.

Fig. 3 also shows the effects of omitting the cross-modal terms in the generalized force matrix, comparing the results between the complete analyses using Eq. 19(c) and omitting the cross terms (B). It has generally been assumed that the cross-modal terms are insignificant because the mode shapes are, by definition, orthogonal. Yip and Flay (1995) suggested that although the mode shapes are orthogonal, the inclusion of the coupled wind forces may change this characteristic. Comparison between results (B) and (C) suggests that the cross modal terms are not always significant. In the cases where they have an effect, they tend to re-distribute the energy among coupled directions, increasing the response in the y direction while decreasing the response in the torsion direction, and vice versa. This could also be a function of the closeness of the periods for the coupled directions. Additional analysis has been carried out using the same aerodynamic data and methodology but with slightly more separated 2nd and 3rd mode periods; i.e., 8.6, 7.1 and 6.5 seconds respectively. Fig. 4 shows that for the y direction, the cross modal terms have a strong effect when the frequencies of the coupled modes are close but they become insignificant when the frequencies are separated. Results for torsion is more mixed with both the cross modal terms and the closeness of the frequencies playing a role in the overall difference.

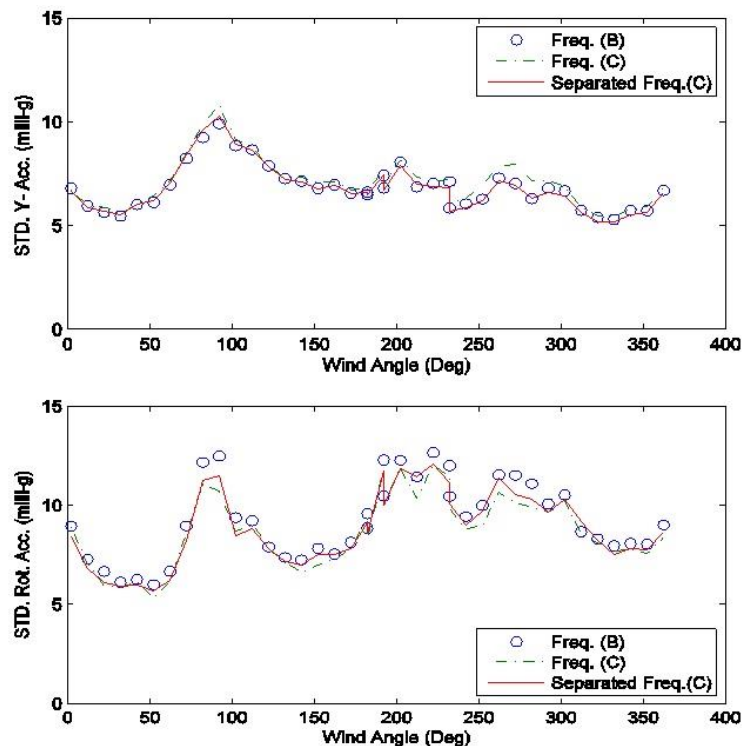


Fig. 4 Effect of separation of the natural frequencies in y and torsion coupled modes

7. Conclusions

This paper provides some historical perspective of the components in the force balance data analysis and discusses some recent developments. Complete formulations of dynamic analysis of wind loads in frequency and time domains are presented which can also be applied to complex structural systems with some additional consideration in the determination of the overall generalized forces in the system. An example has been given to show the effects of omission of correlation terms in the directional wind forces.

References

- American Society of Civil Engineers (2010), *Minimum design loads for buildings and other structures*, ASCE Standard ASCE/SEI 7-10.
- Boggs, D.W. and Peterka, J.A. (1989), "Aerodynamic model tests of tall buildings", *J. Eng. Mech. - ASCE*, **115**(3), 618-635.
- Boundary Layer Wind Tunnel Laboratory (2007), Wind tunnel testing: a general outline.
- Chen, X. and Kareem, A. (2005), "Coupled dynamic analysis and equivalent static wind loads on buildings with three-dimensional modes", *J. Struct. Eng. - ASCE*, **131**(7), 1071-1082.
- Der Kiureghian, A. (1980), "Structural response to stationary excitation", *J. Eng. Mech. - ASCE*, **106**(6), 1195-1213.
- Holmes, J.D. (1987), "Mode shape corrections for dynamic response to wind", *Eng. Struct.*, **9**, 210-212.
- Holmes, J.D., Rofail, A. and Aurelius, L. (2003), "High-frequency base balance methodologies for tall buildings with torsional and coupled resonant modes", *Proceedings of the 11th Int. Conf. on Wind Eng.*, Copenhagen, Denmark.
- Irwin, P., Garber, J and Ho, E. (2005), "Integration of wind tunnel data with full scale wind climate", *Proceedings of the 10th Americas Conference on Wind Engineering*, Baton Rouge, Louisiana, May 31 - June 4.
- Irwin, P.A. and Xie, J. (1993), "Wind loading and serviceability of tall buildings in tropical cyclone regions", *Proceedings of the 3rd Asia-Pacific Symp. on Wind Eng.*, Univ. of Hong Kong.
- Isyumov, N. (1993), "Criteria for acceptable wind-induced motions of tall buildings", *Proceedings of the International Conference on Tall Buildings*, Council of Tall Buildings and Urban Habitat, Rio de Janeiro. May 17-19.
- Isyumov, N. (2002), Private communications.
- Lieblein, J. (1974), *Efficient methods of extreme-value methodology*, Report NBSIR 74-602, National Bureau of Standards, Washington, D.C.
- Standards Australia / Standards New Zealand (2011), Australia / New Zealand Standard, Structural design actions – Wind actions. Part 2. AS/NZS 1170.2:2011.
- Tschanz, T. (1982), *The base balance measurement technique and application to dynamic wind loading of structures*, Ph.D. Thesis, University of Western Ontario, Faculty of Engineering Science, London, Ontario.
- Xie, J. and Irwin, P.A. (1998), "Application of the force balance technique to a building complex", *J. Wind Eng. Ind. Aerod.*, **77-78**, 579- 590.
- Xu, Y.L. and Kwok, K.C.S. (1993), "Mode shape corrections for wind tunnel tests of tall buildings", *Eng. Struct.*, **15**, 618-635.
- Vickery, B.J., Undated Boundary Layer Wind Tunnel Laboratory notes.
- Vickery, P.J., Steckley, A., Isyumov, N. and Vickery, B.J. (1985), "The effect of mode shape on the wind-induced response of tall buildings", *Proceedings of the 5th US Nat. Conf. on Wind Eng.*, Lubbock, Texas, 1B/41-48.

Yip, D.Y.N. and Flay, R.G.J. (1995), "A new force balance data analysis method for wind response predictions of tall buildings", *J. Wind Eng. Ind. Aerod.*, **54-55**, 457-471.

Nomenclature

The following symbols are used in this paper:

- A** state matrix with the size of $2n \times 2n$
- a_{\max} the largest component among the directional accelerations
- a_{\min} smaller component among the directional accelerations
- $a_{\min 1}, a_{\min 2}$ the smaller components among the directional accelerations
- a_{ik} maximum amplitude of the mode at the top of the building to the direction i ($=1$ to 6) of mode k ($=1$ to n)
- a_r resultant acceleration
- B** input matrix: $[2n \times n]$
- C** output matrix: $[9 \times 2n, \text{ or } 15 \times 2n]$
- c_i load combination factors for $i = x, y$ and torsional directions
- $\tilde{\mathbf{C}}$ modal damping matrix with the size of $[n \times n]$
- D** feed forward matrix $[9 \times n, \text{ or } 15 \times n]$
- \hat{E} the predicted load effect
- F** base moment and force column vector with the size of 6
- f** force column vector with the size of $6l$
- \mathbf{f}_i force column vector with the size of l for degree of freedom $i=1$ to 6
- \mathbf{F}_r resonant base force column vector
- F_1, F_2 x_1 and x_2 directional shear forces
- F_3 vertical base force which is generally ignorable in wind force assessment
- F_4, F_5 based bending moments along the axis x_1 and x_2 , respectively
- F_{1r}, F_{2r} resonant base shears along the x_1 and x_2 axes
- $F_{3r} \equiv 0$
- F_{4r}, F_{5r} resonant base moments along the x_1 and x_2 axes
- F_{6r} resonant part of base torque
- \mathbf{f}'_j effective static load distribution vector in load direction j
- \hat{F}_{it} peak base forces (and moments) including resonant component mode 1 to i
- g_q peak factor for the quasi-steady components
- g_r peak factor for the resonant components
- H height of the building
- $\tilde{\mathbf{K}}$ modal stiffness matrix with the size of $[n \times n]$
- l number of lumped masses

$\tilde{\mathbf{M}}$	modal mass matrix with the size of $[n \times n]$
\hat{M}_x	predicted peak base moment M_x
\hat{M}_y	predicted peak base moment M_y
\hat{M}_t	predicted peak base torque M_t
\mathbf{N}	influence matrix to form the base moment and forces from level by level forces (size= $[6 \times 6l]$)
n	total number of modes
\mathbf{Q}	mode shape matrix with the size of $[6 \times n]$ at the elevation z_c
\mathbf{q}	mode shape matrix with the size of $[6l \times n]$
\mathbf{q}_B	matrix with the size of $[n \times 6]$ which formulates the modal loads from base forces / moments
q_{cij}	mode shape value of i-direction of mode j at the elevation z_c
\mathbf{q}_F	matrix with the size of $[6l \times n]$ which formulates the modal loads from floor-by-floor forces
$S_{F_i}(f)$	power spectrum density of the resonant component of base force/moment i
$S_{\mathbf{f}}(f)$	$[n \times n]$ -size cross spectral matrix of the modal load
$S_{\tilde{\mathbf{y}}}(f)$	$[n \times n]$ -size cross spectral matrix of the generalized coordinate $\tilde{\mathbf{y}}$
$S_{\dot{\tilde{\mathbf{y}}}}(f)$	$[n \times n]$ -size cross spectral matrix of $\dot{\tilde{\mathbf{y}}}$
$S_{\ddot{\tilde{\mathbf{y}}}}(f)$	$[n \times n]$ -size cross spectral matrix of $\ddot{\tilde{\mathbf{y}}}$
\mathbf{T}	$[3 \times 3]$ matrix transforms the center displacements to those at (x_1, x_2)
w_{jq}	weighting factor to determine the effective static load shape for quasi-steady component in load direction j
w_{jr}	weighting factor to determine the effective static load shape for resonant component in load direction j
\mathbf{y}	displacement column vector with the size of 6 times the number of lumped masses (l)
\mathbf{y}_i	displacement column vector with the size of l for degree of freedom $i=1$ to 6
\mathbf{z}	elevation column vector with the size of l
$\tilde{\mathbf{y}}$	generalized coordinate
$\dot{\tilde{\mathbf{y}}}$	first order time derivative of generalized coordinate
$\ddot{\tilde{\mathbf{y}}}$	second order time derivative of generalized coordinate
z_c	elevation where the corner accelerations are calculated
γ_i	relative influence coefficients for the pseudo load effect for $i=x, y$ and torsional directions

- v_i cycling rate of the base force/moment component i
- $\sigma_{F_{ir}}$ standard deviation of resonant component of base force/moment F_{ir}
- σ_{F_q} standard deviation of quasi-steady base force/moment
- Ψ_{qj} quasi-steady component of effective load shape for load direction j
- Ψ_{rj} resonant component of effective load shape for load direction j